



Shunt Resistance of a Parallel Vertical Junction Silicon Solar Cell under Monochromatic Illumination and Under Irradiation: Temperature and Wavelength Effects

Alioune Badara Dieng¹, Fakoro Souleymane Dia², Senghane Mbodji², Birame Dieng²

¹Faculty of Science and Technology, University Cheickh Anta Diop, Dakar, Senegal

²Physics Department, Alioune Diop University, Bambey, Senegal physics department, Alioune Diop University, Bambey, Senegal

e-mail: aliounebadara1977@yahoo.fr; fakorosdia@gmail.com; senghane.mbodji@uadb.edu.sn
biram.dieng@uadb.edu.sn

Abstract In this paper, we made a theoretical study of a parallel vertical junction solar cell under monochromatic illumination, in static mode and under irradiation.

The resolution of the continuity equation that governs the generation, the recombinations and the process of diffusion of the electrons in the base, helped us to establish the expression of the electrons density in the base and deduce expressions of the photocurrent density and the phototension depending on the wavelength λ , the recombination velocity at the junction S_f and the temperature.

The expression of Shunt resistance has been established from those of phototension and photocurrent density.

We studied the influence of temperature and wavelength variations on the minority carriers density in the base, the photocurrent density, the phototension and finally on the Shunt resistance.

Keywords Silicon solar cell, Temperature, Wavelength, Shunt resistance

1. Introduction

We will perform, through this paper a theoretical study of a parallel vertical junction solar cell under monochromatic illumination, in static mode and under irradiation.

The resolution of the continuity equation will enable us to establish the expression of the minority density charge carriers in the base and deduce those of the photocurrent density and the phototension.

The expression of the Shunt resistance will be subsequently obtained.

We will study, in this article, the impact of the change in temperature and the wavelength on the density of the minority carriers in the base, the photocurrent density, the phototension and finally on the Shunt resistance.

2. Theory

We consider a n^+p-p parallel vertical junction solar cell whose structure can be represented as follows:

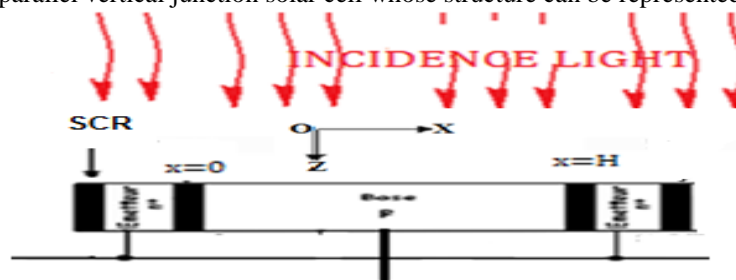


Figure 1: Parallel vertical junctions of a solar cell



When the solar cell is illuminated, there is a creation of electron-hole pairs in the base.

The behaviour of the minority carriers in the base (the electrons) is governed by the continuity equation which integrates all the phenomena causing the variation of the density of the electrons according to the width x of the base, its depth z , the recombination velocity at the junction, of the wavelength, temperature and irradiation parameters.

The resolution of this equation will enable us afterwards to express on the one hand the density minority charge carriers from the base and deduce those of the quantities and other solar cell electrical parameters.

The continuity equation in static mode is presented in the form below:

$$D(T) \cdot \frac{\partial^2 \delta(x, kl, \phi, \lambda, z, T)}{\partial x^2} - \frac{\delta(x, kl, \phi, \lambda, z, T)}{\tau(kl, \phi)} = -G(z, \lambda) \quad (1)$$

$\delta(x, kl, \phi, \lambda, z, T)$ describes the density of minority carriers in photo-generated charge.

$D(T)$ is the coefficient diffusion according to the temperature. It is obtained by Einstein relationship:

$$D(T) = \mu(T) \frac{k_b}{e} \cdot T \quad (2)$$

$\mu(T)$ denotes the mobility of the charge carriers according to the temperature.

$$\mu(T) = 1,43 \cdot 10^9 T^{-2,42} \text{ cm}^2 \cdot \text{V}^{-1} \cdot \text{S}^{-1}$$

$\tau(kl, \phi)$ is the average lifetime of carriers according to irradiation parameters.

We have the relationship:

$$\frac{1}{\tau(kl, \phi)} = \frac{1}{\tau_0} + kl\phi \quad [1]$$

kl and ϕ respectively denote the damage coefficient and the irradiation energy. τ_0 is the average lifetime of carriers with the absence of irradiation.

$G(z, \lambda)$ is the overall generation rate of the minority charge carriers according to the depth z of the base and wavelength.

The continuity equation can be written again as follows:

$$\frac{\partial^2 \delta(x)}{\partial x^2} - \frac{\delta(x)}{L^2} + \frac{G(z, \lambda)}{D} = 0 \quad (3)$$

$$L(kl, \phi, T) = \sqrt{D(T) \times \tau(kl, \phi)} \quad (4)$$

is the diffusion length.

The expression of the overall generation of minority charge carriers' rate is of the form: [2]

$$G(z, \lambda) = \alpha_i (1 - R(\lambda)) \cdot F \cdot \exp(-\alpha_i \cdot z) \quad (5)$$

$R(\lambda)$ is the monochromatic reflection coefficient; F is the flux of incident photons resulting from a monochromatic radiation. α is the coefficient of monochromatic absorption.

$$\frac{\partial^2 \delta(x)}{\partial x^2} - \frac{\delta(x)}{L^2} = -\frac{G(z, \lambda)}{D} \quad (6)$$

2.1. Solution of the continuity equation

- Special solution:

$$\delta_1(x) = \frac{L^2}{D} \alpha(\lambda) (1 - R(\lambda)) \cdot F \cdot \exp(-\alpha_i \cdot z) \quad (7)$$

-solution of the second member equation:

$$\delta_2(x) = A \cosh\left(\frac{x}{L}\right) + B \sinh\left(\frac{x}{L}\right) \quad (8)$$



-thus, the general solution is:

$$\delta(x, z, \lambda, Sf, kl, \phi, T) = \left[A \cosh\left(\frac{x}{L(kl, \phi, T)}\right) + B \sinh\left(\frac{x}{L(kl, \phi, T)}\right) + \frac{L^2(kl, \phi, T)}{D(T)} \cdot \alpha(\lambda)(1 - R(\lambda)) \cdot F \cdot \exp(-\alpha, z) \right] \quad (9)$$

2.2. Find the coefficients A and B

- The boundary conditions:

-Therefore, in the junction (x = 0) we have:

$$D(T) \cdot \left. \frac{\partial \delta(x_i, z_i, \lambda, kl, \phi, T)}{\partial x} \right|_{x=0} = Sf \cdot \delta(x_i, z_i, \lambda, kl, \phi, T)|_{x=0} \quad (10)$$

Sf is the recombination velocity at the junction. This phenomenological parameter describes how the base minority carriers go through the junction. It can be divided into two terms [3].

We have $Sf = Sf_o + Sf_j$

Sf_o induced by the shunt resistance, is the intrinsic recombination velocity. It depends only on the intrinsic parameters of the solar cell.

Sf_j reflects the current which is imposed by an external charge and thus defining the operating point of the solar cell

-At The middle of the base: ($x = \frac{H}{2}$) .The structure of the solar cell, with two similar junctions on either side of the base, portends the equation (9) below:

$$D(T) \cdot \left. \frac{\partial \delta(x, z, kl, \lambda, \phi, T)}{\partial x} \right|_{x=H/2} = 0 \quad (11)$$

H is the thickness of the solar cell's base.

3. Results and Discussion

3.1. Density profile minority charge carriers in the base

Figure 2 below shows the profile of the electron density in the base according to the wavelength for different values of the temperature.

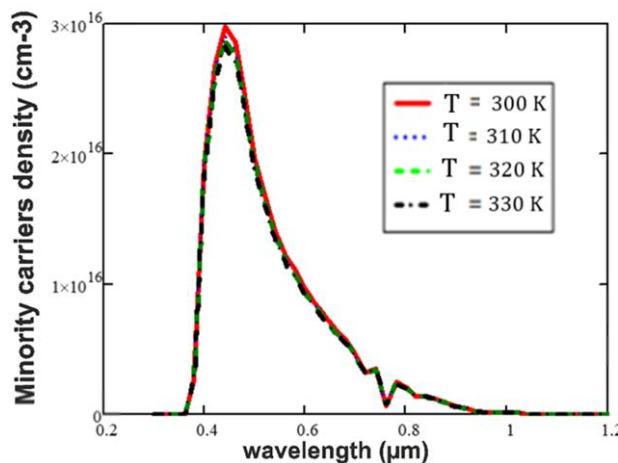


Figure 2: Variation of the minority carriers density according to the wavelength for different values of the temperature.

$H=0,03cm, Z=0,0001cm, L_o=0,01cm, kl = 10 cm^2/s, \phi=50MeV$

The analysis of the curves shows that the minority carriers charges density in the base increases according to the wavelength in the interval [0.40 μm; 0.50μm] and progressively decreases in the rest of the visible spectrum by undergoing slight fluctuations around λ = 0.8 μm.

The minority carrier charges density in the base decreases when the incidence angle of solar radiation increases. The majority of photons emitted by the sun are in the visible domain and the charge carriers density depends on the photon flux of the solar radiation, which increases according to the wavelength up to the peak λ = 0.5 μm and then decreases progressively with small variations noted towards the end of the visible spectrum.

In the interval [0.40 μm; 0.50 μm], the generation of carriers is very high with sufficiently energetic photons absorbed near the illuminated surface and the surface recombinations are weak.

The decrease of the minority carrier density result from that of the photons flux which are less and less energetic.

The photogenic carriers have less and less energy and the volume recombinations combined to that surface reduce the density.

Indeed low energy photons are absorbed in volume and it must take into account the phenomena of luminous wave's attenuation.

The temperature' increase reduces the mobility of the charge carriers that promotes recombinations, which results in the decrease of the minority charge carriers' density.

3.2. Photocurrent density profile

The expression of the photocurrent density of the solar cell is obtained from the gradient of the minority carriers' density in the base according to Fick's law. We have:

$$J_{ph} = 2q D(T) \cdot \left. \frac{\partial \delta(x, z, \lambda, kl, \phi, T)}{\partial x} \right|_{x=0} \tag{12}$$

Where q is the elementary charge of electricity. From where:

$$J_{ph} = 2q \frac{S_f L^3 \cdot \alpha_i (1 - R) \cdot F \cdot \exp(-\alpha_i \cdot z) \cdot \tanh\left(\frac{H}{2L}\right)}{S_f \cdot L + D \tanh\left(\frac{H}{2L}\right)} \tag{13}$$

Figure 3 below shows the profile of the photocurrent density according to the wavelength for different values of temperature.

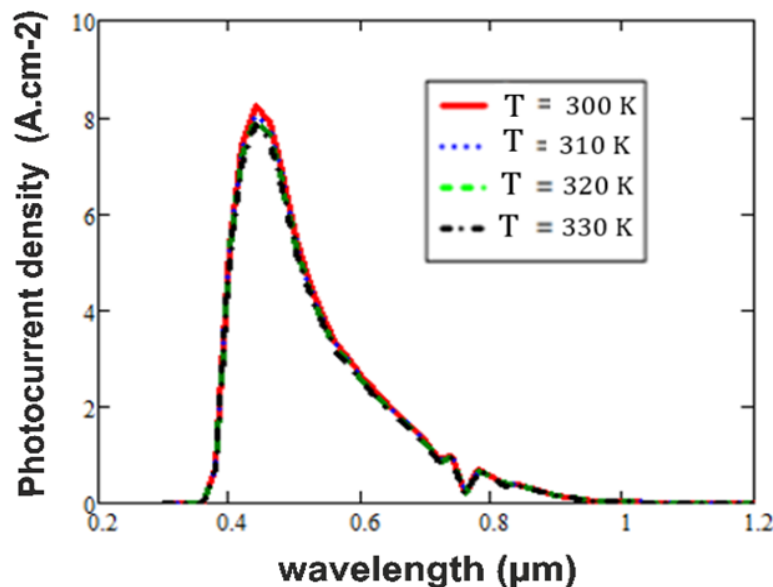


Figure 3: Variation of the photocurrent density according to the wavelength for different values of the temperature

$$H=0, 03cm, Z=0, 0001cm, L_o=0, 01cm, kl = 10 \text{ cm}^2/s, \phi=50MeV$$

The analysis of the curves shows that the photocurrent density variations according to the wavelength for different temperature values are similar to those of the minority charge carriers density of the base. The contribution of the minority charge carriers from the base in the current delivered by the solar cell is related to the variations of the density of these carriers according to Fick's law.

3.3. Phototension Profile

The phototension created by accumulation of charge carriers at the junction is obtained from Boltzmann's relationship:

$$V = V_T \cdot \ln \left[1 + \frac{N_b}{n_i^2(T)} \cdot \delta(0, z, \lambda, kl, \phi, Sf, T) \right] \tag{14}$$

$V_T = \frac{KT}{e}$ is the thermal tension

N_b : doping rate of acceptor atoms in the base

$n_i(T)$: intrinsic minority carriers density according to the temperature.

$$n_i(T) = A.T^{\frac{3}{2}} \exp\left(\frac{-E_g}{2k_b.T}\right); A \text{ is a coefficient: } A = 3,87.10^{16} \text{ cm}^{-3} \text{ K}^{\frac{-3}{2}} \tag{15}$$

E_g is the gap energy; It correspond at the energy between conduction and valence band. We are

$$E_g = E_c - E_v = 1.12 \text{ eV}$$

From where:

$$V_{ph} = \frac{KT}{q} \ln \left\{ 1 + \frac{N_b}{n_i^2} \left[\frac{D \tanh\left(\frac{H}{2L}\right)}{S_1 L + D \tanh\left(\frac{H}{2L}\right)} \right] \cdot \frac{L^2}{D} \cdot \alpha_i (1-R) \cdot F \cdot \exp(-\alpha_i \cdot z) \right\} \tag{16}$$

Figure 4 below shows the profile of the phototension according to the wavelength for different values of the temperature.

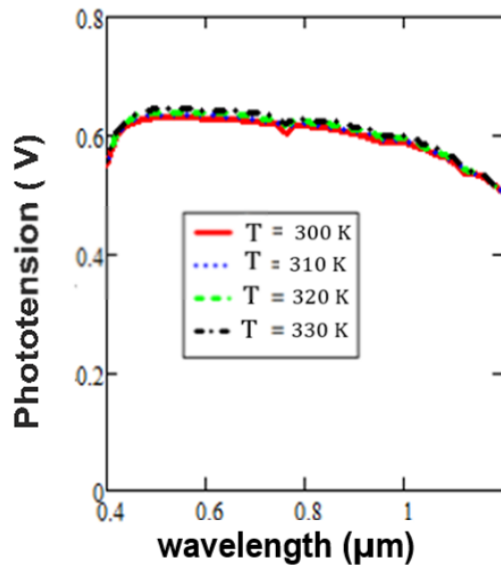


Figure 4: Variation of the phototension according to the wavelength for different values of the temperature.

$$H=0, 03\text{cm}, Z=0, 0001\text{cm}, L_o=0, 01\text{cm}, kl = 10 \text{ cm}^2/\text{s}, \phi=50\text{Mev}$$

The variations of the phototension according to the wavelength for different values of the temperature follow the same trends as those of the minority carrier density in the base.

The phototension increase according to the temperature.



The reduced mobility of charge carriers combined with their thermal generation because of the temperature increase creates a growth of the quantities of charges stored on either side of the junction.

3.4. Current-voltage characteristic:

Figure 5 below shows the profile of photocurrent density according to the phototension.

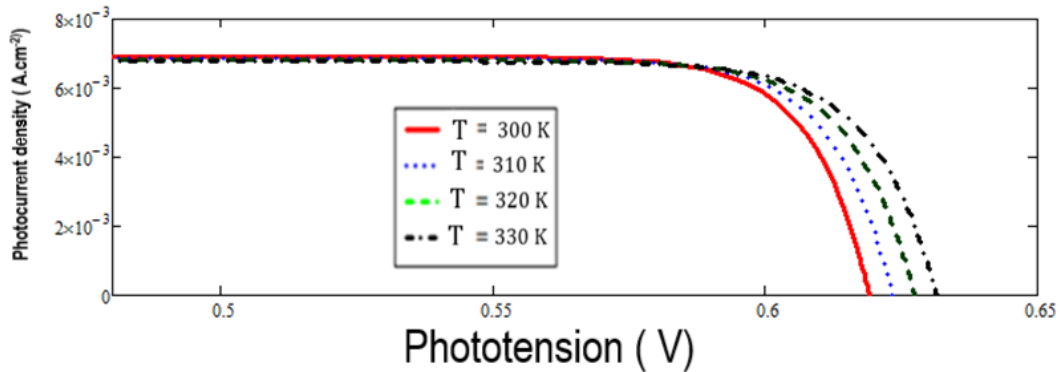


Figure 5: I-V characteristic of the solar cell

The characteristic analysis shows that the phototension is not independent of the photocurrent. The solar cell operates as a real voltage generator in the vicinity of the open circuit and as a real current generator near the short circuit.

For each mode of operation, an electrical circuit equivalent to the solar cell is proposed.

Below is the electric model, which is equivalent to the solar cell and operating as a real current generator:

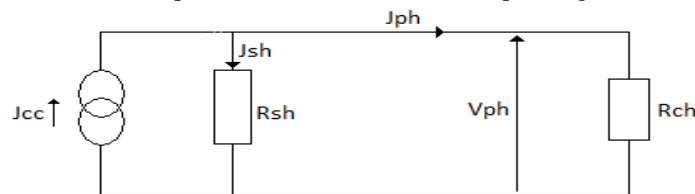


Figure 6: Equivalent circuit of the solar cell (real current generator)

From the study of this electrical circuit, the expression of the shunt resistance deduced:

$$R_{SH}(S_f, \lambda, kl, \phi, z, T) = \frac{V_{PH}(S_f, \lambda, kl, \phi, z, T)}{J_{CC}(\lambda, kl, \phi, z, T) - J_{PH}(S_f, \lambda, kl, \phi, z, T)} \tag{17}$$

Figure 5a below represent the profile of the Shunt resistance according to the wavelength for different values of the temperature.

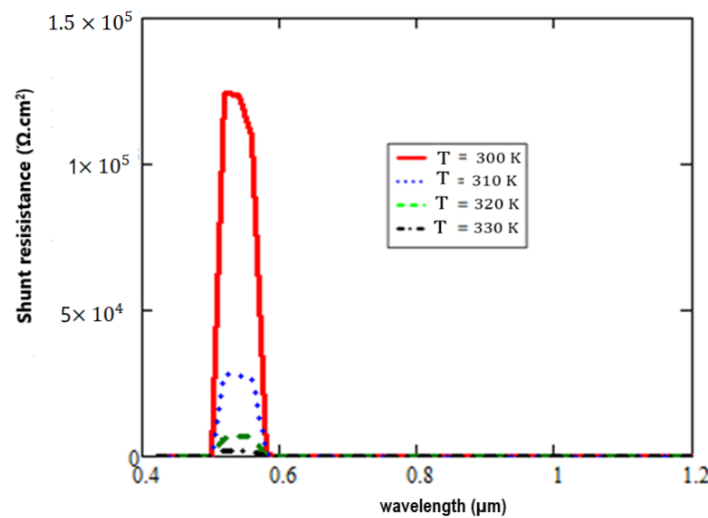


Figure 7: Variation of the Shunt resistance according to the wavelength for different values of the temperature
 $H=0, 03cm, Z=0, 0001cm, L_o=0, 01cm, kl = 10 \text{ cm}^2/s, \phi=50MeV, S_f = 6.10^6 \text{ cm/s}$

The volume, surface and interface recombinations (base-emitter, base-contact, and contact-emitter) create the Shunt resistance, which models the leakage currents in the solar cell.

The analysis of the curves shows that Shunt resistance increases with wavelength in the range [0.40 μm ; 0.50 μm], and then decreases in the rest of the visible spectrum.

When the wavelength grows, the photocurrent density increases in the interval [0.40 μm ; 0.50 μm], which means that the leak currents decrease, hence the growth of shunt resistance.

In the rest of the visible spectrum, we are noted opposite effects.

Shunt resistance decreases when the temperature increase because the growth of the temperature favors parasitic currents, which explains the decrease of the Shunt resistance.

4. Conclusion

The resolution of the continuity equation allowed us to obtain the expression of electron density in the base and we deduced those of photocurrent density and phototension.

From the electric model equivalent to the solar cell when it operates in the vicinity of the short circuit, we established the expression of the Shunt resistance.

We studied in this article the impacts of variations in wavelength and temperature on the density of minority carriers in the base, photocurrent density, phototension and finally on Shunt resistance.

The study showed that variations in temperature and wavelength influence Shunt resistance.

The temperature's increase results in a decrease of the charge carriers density, photocurrent density, Shunt resistance and increase of the phototension.

The study showed that variations in temperature and wavelength influence Shunt resistance.

Thermal generation, combined with reduced charge carriers' mobility, which promotes recombinations and leakage currents, explains the decrease of the charge carriers density and Shunt resistance.

This reduced mobility of the carriers causes an increasing accumulation of charges on either side of the junction.

The charge carriers' density, the photocurrent density, the phototension and the Shunt resistance increases with the wavelength in the interval [0.40 μm ; 0.50 μm].

In the rest of the visible spectrum, we are noted adverse effects due to the decline of the generation rate and the increase of parasitic currents.

References

- [1]. Kraner. H. W. (1983), Radiation damage in silicon detectors, 2nd Pisa meeting on Advanced Detectors, Grosseto, Italy, June 3-7.
- [2]. Bousse. L, Mostarshed. J., Hafeman. D, Jurtor. M., Adami. M and Nicolini. C. (1994), Investigation of carrier transport through silicon wafers by photocurrent measurements, J. App. Phys. Vol 75(8), pp. 4000-4008.
- [3]. H.L. Diallo, A.S. Maiga, A. Wareme and G. Sissoko. (2008), New approach of both junction and back surface recombination velocities in a 3D modelling study of a polychristalline silicium solar cell, J. App. Phys., Vol 42, pp. 203-211.
- [4]. Hu, CC. (2010), Modern semi-conductor devices for integrated circuits, Pearson/ Prentice Hall, New jersey
- [5]. M. Ndiaye, A. Diao, M. Thiame, M.M. Dione, H.L. Diallo, M.L. Samb, I. Ly, C. Gassama, S. Mbodj F. I. Barro and G. Sissoko. (2010), 3D Approach for a modelling study of diffusion capacitance's efficiency of the solar cell, 25th European photovoltaic solar energy conference and exhibition, 5th world conference of photovoltaic energy conversion, Valencia-Spain.
- [6]. Green M.A. (2008). Solar energy. Material and Solar Cells. Vol. 92, 1305–1310.
- [7]. A. Diao, N. Thiam, M. Zoungrana, M. Ndiaye, G. Sahin and G. Sissoko. (2014). Diffusion coefficient in silicon solar cell with applied magnetic field and under frequency: Electric equivalent circuits, World Journal of Condensed Matter Physics, 4(5), 84-92.
- [8]. A. Dieng, M.L. Sow, S. Mbodji, M.L. Samb, M. Ndiaye, M. Thiame, F.I. Barro and G. Sissoko. (2009). 3D study of a polycrystalline silicon solar cell: Influence of applied magnetic field on the



- electrical parameters, Proceedings of the 24th European Photovoltaic Solar Energy Conference and Exhibition, Hamburg, Germany, 473-476.
- [9]. M.I. Ngom, B. Zouma, M. Zoungrana, M. Thiame, Z.N. Bako, A.G. Camara and G. Sissoko. (2012). Study of a solar cell with parallel vertical junction for static regime under polychromatic illumination and magnetic field: Influence of the magnetic field on the electric parameters, *International Journal of Advanced Technology & Engineering Research (IJATER)*, 2(6), 101-109.
- [10]. S. Madougou, F. Made, M. S. Boukary, and G. Sissoko. (2007). I-V Characteristics for Bifacial Silicon Solar Cell studied under a Magnetic field. *Advanced Materials Research Vols. 18-19 pp. 303-312*, online at <http://www.scientific.net> © Trans Tech Publications, Switzerland - ISSN: 1022-6680 and ISBN: 0-87849-450-2d.
- [11]. B. Equer, (1993). "Energie solaires photovoltaïque", Volume 1, Collection Ellipses.
- [12]. R.M. Lago-Aurrekoetxea, C. del Cañizo, I. Pou, and A. Luque. (2001). "Fabrication process for thin silicon solar cells", *Proc. 17th European PVSEC*, 1519-1522.
- [13]. N. Bordin, L. Kreinin, N. Eisenberg. (2001). Determination of recombination parameters of bifacial silicon cells with a two layer step-liked effect distribution in the base region", *Proc.17th European PVSEC*, 1495-1498.
- [14]. Daniel. L. Meier, Jeong-Mo Hwang, Robert B. Campbell. (1988). *IEEE Transactions on Electron Devices*, vol. ED-35, No. 1, pp. 70–78.
- [15]. Jose Furlan and Slavko Amon. (1985). "Approximation of the carrier generation rate in illuminated silicon", *Solid State Electr*, Vol. 28, No. 12, pp. 1241-1243.

